Limnol. Oceanogr., 53(1), 2008, 122–136

Dissolved organic matter and bacterial production and respiration in the sea–surface microlayer of the open Atlantic and the western Mediterranean Sea

Thomas Reinthaler,[1] *Eva Sintes, and Gerhard J. Herndl*
Department of Biological Oceanography, Royal Netherlands Institute for Sea Research (NIOZ), P.O. Box 59, 1790 AB Den Burg, Texel, The Netherlands

Abstract

The sea–surface microlayer (SML) is the boundary layer between the ocean and the atmosphere. We measured bacterial production and respiration along with dissolved organic carbon (DOC), nitrogen (DON), and phosphorus, inorganic nutrients, and dissolved amino acids in the SML and the underlying water (ULW) of the subtropical Atlantic gyre (SATL) and the western Mediterranean Sea (WMED). Dissolved amino acid concentrations in the SML were one order of magnitude higher than in the ULW. DON, ammonium, and nitrate were also significantly enriched in the SML as compared with the ULW. Bacterial leucine incorporation ranged between 3 and 50 pmol L^{-1} h^{-1} in the SATL and 5 and 488 pmol L^{-1} h^{-1} in the WMED and was generally not significantly different between the SML and the ULW. In contrast, bacterial respiration was significantly higher in the SML than in the ULW, varying between 3.6 and 9.5 μmol L^{-1} d^{-1} O_2 at both sites. The resulting bacterial growth efficiencies ranged between 0.1% and 14% using different leucine incorporation to carbon conversion factors. Given the high dissolved free amino acid (DFAA) yield of DOC (~12%) and of DON (~30%) in the SML, bacterial growth efficiencies in the SML were low. This indicates that the DFAA in the SML are not readily available for bacteria. The underlying mechanisms of this immobilization of DFAA in the SML and their production remain enigmatic.

The sea–surface microlayer (SML) is the boundary layer between the atmosphere and the oceans covering ~70% of the earth's surface. Although the thickness of the SML is only about 10–250 μm, this interface is important in mediating the exchange of gases and organic and inorganic matter between the atmosphere and the bulk surface waters (Liss and Duce 1997).

It is well established that the SML is a unique environment with considerable variability in chemical and biological characteristics compared with the underlying waters (ULW). Dissolved compounds such as nutrients, dissolved organic carbon (DOC), and amino acids are often enriched in the SML, especially in the visible slicks of near-shore environments (Williams et al. 1986). The enrichment of these compounds in the SML has been attributed to surface-active matter collected by rising gas bubbles in the upper water column (Kuznetsova and Lee 2002) or by Langmuir circulations in the open ocean (Hardy 1982). Atmospheric deposition of matter might be important for the development of a SML as well (Wotton and Preston 2005).

Despite the long-lasting interest in the physicochemical properties of the SML, studies on the microbial metabolism in the SML are still scarce, particularly for open oceans comprising the vast majority of the oceans' surface. For microbes, however, the SML might be a stressful environment. The SML receives intense solar irradiation, especially in the low wavelength range of ultraviolet-B (300–320 nm), which is detrimental to organisms (Regan et al. 1992). Nevertheless, distinct bacterioneuston communities and higher activities of the neuston than of the plankton community below the SML have been reported for coastal systems (Carlucci et al. 1985; Agogué et al. 2004; Joux et al. 2006).

The main function of heterotrophic bacteria in the carbon cycling is the production of biomass and the remineralization of DOC to CO_2 (Del Giorgio and Cole 2000). The bacterial growth efficiency (BGE) relates biomass production to the bacterial uptake of DOC. Enhanced respiration rates in the SML have been measured in various environments. Most of these measurements were not direct oxygen consumption or CO_2 production measurements, however, but used either radiolabeled organic model compounds or electron transport system estimates (De Souza Lima 1985; Mimura et al. 1988). The only study directly measuring oxygen consumption of the total microbial community in the SML at a coastal site also found high rates of carbon remineralization (Obernosterer et al. 2005). For the open-ocean SML, respiration measurements of prokaryotic communities are not available. The global extension of the open-ocean SML suggests, however, that the metabolic activity of the SML community might influence the exchange of gases between the ocean and the atmosphere. In a gradient from high- to low-productivity North Atlantic waters, a strongly negative relationship between net community production and CO_2 fluxes in the top 2-cm layer has been reported (Calleja et al.

[1] Corresponding author (thomas.reinthaler@nioz.nl).

Acknowledgments

We thank the captain and crew of the RV *Pelagia* for their support at sea. Special thanks go to K. Bakker, S. Gonzalez, and A. Smit for the DON and DOP, DOC, and amino acid analysis, respectively. Helpful comments and suggestions from two anonymous reviewers are gratefully acknowledged.

The BADE cruises were funded by the Dutch Science Foundation (NWO-ALW), project 812.03.001 to G.J.H.

This research is a contribution to the Networks of Excellence of the EU FP6 MarBef and Eur-Oceans.

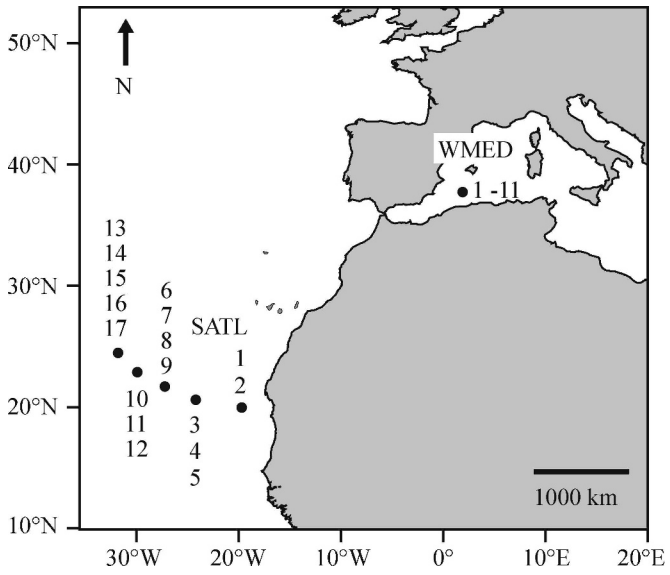

Fig. 1. Map of the study area in the subtropical Atlantic (SATL) and the western Mediterranean Sea (WMED). In the SATL, a transect from the highly productive Mauritanian upwelling area into the oligotrophic gyre was followed. In the WMED, a stable anticyclonic eddy system was sampled over a 2-week period. Circles and numbers indicate the individual stations occupied.

2005). This suggests substantial biological control of the exchange of CO_2 across the air–sea interface.

In this study, we aimed at determining the spatial and temporal variability of selected biological and chemical parameters of the SML in the open eastern North Atlantic and the western Mediterranean Sea. In the North Atlantic, a gradient was followed from the highly productive Mauritanian upwelling system to the subtropical North Atlantic (SATL) gyre. The other sampling site was located in the Algerian basin of the western Mediterranean Sea (WMED), where we followed the biological dynamics in a stable anticyclonic eddy system over time. We found that dissolved free amino acids (DFAA), commonly efficiently utilized by bacteria, were present at high concentrations in the SML. BGEs, however, were lower in the SML than in the underlying bulk water in the SATL and similar in the western Mediterranean eddy.

Methods

Study sites and sampling—Samples of the SML and the ULW were collected at two open-ocean sites. In the eastern SATL, we followed a transect from the productive Mauritanian upwelling region (20°25′N, 18°10′W) into the oligotrophic gyre (24°39′N, 31°10′W; Fig. 1) during Sep–Oct 04. In the Algerian basin of the WMED, we investigated a stable anticyclonic eddy system (at 37°50′N and 2°05′E) for a period of 3 weeks in Sep–Oct 03 (Fig. 1). To track the eddy, a drifting buoy was deployed in the center of the eddy and sampling took place within 500 m of the buoy. The positions of the individual sampling stations for the two sites and the time of sampling are given in Table 1.

Table 1. Overview on the sampling positions, dates, and time of visited stations (STN) in the subtropical Atlantic (SATL) and the western Mediterranean (WMED).

STN	Date	Time (local)	Lat (°N)	Long (°W)
		SATL		
1	25 Sep 04	07:45	20.03	19.27
2	25 Sep 04	13:15	20.03	19.27
3	29 Sep 04	08:30	20.69	24.06
4	29 Sep 04	13:15	20.69	24.06
5	29 Sep 04	17:00	20.69	24.06
6	02 Oct 04	13:15	21.77	26.71
7	02 Oct 04	17:00	21.77	26.71
8	03 Oct 04	08:00	21.76	26.64
9	03 Oct 04	13:15	21.71	26.65
10	05 Oct 04	08:00	23.00	29.39
11	05 Oct 04	13:15	22.97	29.43
12	05 Oct 04	17:00	22.99	29.44
13	07 Oct 04	07:45	24.60	31.24
14	07 Oct 04	13:15	24.58	31.24
15	07 Oct 04	17:00	24.57	31.23
16	08 Oct 04	07:45	24.49	31.25
17	08 Oct 04	10:30	24.47	31.26
		WMED		
1	29 Sep 03	10:00	37.74	-2.02
2	29 Sep 03	15:00	37.76	-2.02
3	29 Sep 03	19:00	37.76	-2.01
4	30 Sep 03	10:00	37.77	-1.98
5	30 Sep 03	16:00	37.80	-1.97
6	30 Sep 03	20:00	37.81	-1.95
7	04 Oct 03	10:00	37.87	-2.15
8	04 Oct 03	15:30	37.87	-2.15
9	05 Oct 03	10:30	37.78	-2.20
10	05 Oct 03	15:30	37.75	-2.20
11	05 Oct 03	19:00	37.72	-2.18

Samples of the SML and the ULW (~30 cm depth) were taken from a drifting inflatable boat upwind of the RV *Pelagia*. If weather permitted, sampling was conducted in the morning, at noon, and in the late afternoon. SML samples were taken with a glass plate sampler (500 mm long, 250 mm wide, 4 mm thick). The glass plate was introduced vertically into the water and gently withdrawn (Harvey and Burzell 1972). To remove excess water, the plate was allowed to drain for ca. 20 s before the plate was inserted into a slot with Teflon wipers on each side. The wiper blades scraped off the SML and collected it in a 1.5-liter glass bottle placed underneath the wiper blades. Per dip, 5–10 mL of SML was collected. Thus, the thickness of the collected SML was between 40 and 80 μm calculated from the volume of the sample divided by the area of the sampler. This estimated SML thickness is in the range of reported values for glass plate samplers (Harvey and Burzell 1972).

The ULW was sampled with a glass bottle filled at 30-cm depth. All the glassware including the glass plate and the Teflon wipers were kept in an acid bath (0.1 mol L^{-1} HCl) until sampling. All the sampling gear was vigorously rinsed with sampling water before sampling. With two glass plate samplers used concurrently, ~3 liters of SML were sampled

within 1.5 h. Back on board the ship, the sample was split for the different parameters and either preserved for later analyses or analyzed immediately as described below. Salinity and temperature data of the near-surface waters were derived from the ship's online monitoring system, pumping water from about 3-m depth through the respective calibrated sensors. Wind speed data were derived from the ship's meteorological monitoring system.

Inorganic nutrients—The methods for determining inorganic nutrient concentrations followed Joint Global Ocean Fluxes Study recommendations (Gordon et al. 1993). The concentrations of dissolved inorganic nutrients (NH_4^+, NO_3^-, NO_2^-, PO_4^{3-}) were determined in a TRAACS autoanalyzer immediately after collecting the samples and gentle filtration through 0.2-μm filters (Acrodisc, Gelman Science). NH_4^+ was detected with the indophenol blue method (pH 10.5) at 630 nm. NO_2^- was detected after diazotation with sulfanilamide and *N*-(1-naphtyl)-ethylene diammonium dichloride as the reddish-purple dye complex at 540 nm. NO_3^- was reduced in a copper cadmium coil to nitrite (with imidazole as a buffer) and then measured as nitrite. Inorganic PO_4^{3-} was determined via the molybdenum blue complex at 880 nm.

Dissolved organic carbon (DOC)—Samples for DOC were filtered through rinsed 0.2-μm polycarbonate filters and sealed in precombusted (450°C for 4 h) glass ampoules after adding 50 μL of 40% phosphoric acid. The samples were stored frozen at −20°C until analysis back in the lab. DOC concentrations of duplicate samples were determined using a Shimadzu TOC-5000 analyzer. Three-point standard curves, prepared with potassium hydrogen phthalate (Nacalai Tesque, Kyoto, Japan), were used to calculate DOC concentrations. The instrument's performance and the validity of the calibration were determined using reference material of the Hansell CRM program (44–46 μmol L^{-1} for the reference samples; $n = 3$ and 1–2 μmol L^{-1} for low carbon water; $n = 3$). The average analytical precision of the instrument was <3%.

Dissolved organic nitrogen (DON) and dissolved organic phosphorus (DOP)—Total dissolved nitrogen (TDN) and total dissolved phosphorus (TDP) were analyzed with a TRAACS 800 continuous-flow analysis system following the persulfate oxidation method. DON concentrations were calculated by subtracting the sum of the inorganic nitrogen species from TDN concentrations. Similarly, DOP concentrations were calculated by subtracting PO_4^{3-} from TDP. The recovery of DON and DOP was estimated on a mixture of 10 different organic compounds containing known concentrations of N and P (Kramer et al. 2005). To increase the recovery of DOP, samples were kept under pressure at 110°C for 90 min instead of 45 min. The recovery efficiency for these model compounds was 101.8% ± 6.9% for DON and 96.0% ± 3.9% for DOP.

Amino acid analysis—Seawater samples were filtered through prerinsed 0.2-μm polycarbonate filters (Millipore GTTP, 25 mm) and subsequently transferred into combusted glass ampoules and stored at −20°C until analysis. The filtration unit and filters were rinsed with 10% HCl and Milli-Q water before filtration. Concentrations of total dissolved hydrolyzable amino acids (THAA) and DFAA were measured by high-performance liquid chromatography (HPLC), separating fluorescent *o*-phthaldialdehyde (OPA) derivatives. For chiral separation, *n*-isobutyryl-L-cysteine (IBLC) was used as thiol group. Our analytical protocol is based on the method described by Fitznar et al. (1999) with some optimization for our system. Analyses were performed on a temperature-controlled Dionex HPLC system, equipped with a guard column (Security Guard, Phenomenex) and a stationary phase column (Syngeri 4μ MAX-RP 80A, Phenomenex). Amino acids were separated with a gradient of sodium acetate (25 mmol L^{-1}, pH 6.0; solvent A) and methanol (Lichrosolv, Merck, HPLC grade, solvent B), starting with 96% A to 40% A at 75 min, then 0% A until 95 min. After 95 min, the system was returned to 96% A and equilibrated for 5 min. The fluorescence was measured at 330 nm excitation and 445 nm emission wavelengths with a RF-2000 fluorescence detector.

For sample hydrolysis, 500 μL of 37% HCl was added to 500 μL of sample in a 2-mL glass vial. Then, 10 μL of ascorbic acid (0.1 mmol L^{-1} final concentration) was added and the mixture was flushed with nitrogen for 10 min, sealed, and kept at 110°C for 20 h. Subsequently, the samples were dried under nitrogen gas (grade 5) and 500 μL of borate buffer (0.5 mol L^{-1}, pH 10.4) was added. Thereafter, the sample was sonicated and after centrifugation at 4,000 × g for 1 min, 250 μL of the supernatant was transferred to a glass insert.

The OPA : IBLC reagent was prepared by dissolving 20 mg of OPA and 48 mg of IBLC in 1.25 mL of methanol and 8.75 mL of borate buffer (1 mol L^{-1}, pH 10.4). Aliquots of the reagent were stored at −20°C in amber glass vials until use. Derivatization took place in the autosampler of the HPLC system, where 30 μL of the OPA : IBLC reagent was added to 100 μL of sample and mixed automatically. Finally, 100 μL of sample was injected into the HPLC system and measured as described above. Dissolved combined amino acids (DCAA) were calculated as the difference between THAA and DFAA. Depending on the method used, a variable fraction of amino acids might isomerize during acid hydrolysis, thus resulting in quantification errors of L and D enantiomers. However, the liquid-phase hydrolysis we used did not result in significant racemization of free amino acids as revealed by previous tests and also reported by Kaiser and Benner (2005).

Bacterial abundance—One-milliliter samples of unfiltered and 0.8-μm-filtered seawater were fixed with filtered paraformaldehyde (1% final concentration) for 10 min. Subsequently, the samples were stained with SYTO Green (Molecular Probes, 5 μmol L^{-1} final conc.) at room temperature in the dark for 10 min. Analyses were done on a FACSCalibur flow cytometer (BD Biosciences). Counts were performed with the argon laser at 488 nm set at an energy output of 15 mW. Cells were enumerated according to their right-angle light scatter and green

fluorescence measured at 530 nm. To calibrate the system, a known concentration of beads was counted with the flow cytometer and cross-checked by epifluorescence microscopy.

Leucine incorporation rates and bacterial production—Leucine incorporation rates in unfiltered and 0.8-μm-filtered seawater were measured by [^{3}H]-leucine incorporation (specific activity: 5.809 TBq mmol^{-1} for the WMED and 5.920 TBq mmol^{-1} for the SATL; final concentration 10 nmol L^{-1}). A 1 : 1 mixture of hot : cold leucine was added. Two 5-mL samples and one blank were incubated in the dark. The blank was fixed immediately with concentrated 0.2-μm-filtered formaldehyde (4% final concentration, v/v) 10 min before adding the tracer. After incubating the samples and the blank at in situ temperature for 0.5–1.5 h, depending on the expected activity, the samples were fixed with formaldehyde (4% final concentration), filtered onto 0.2-μm polycarbonate filters (Millipore GTTP, 25 mm diameter) supported by a Millipore HA cellulose nitrate filter, and rinsed twice with 10 mL of ice-cold 5% trichloroacetic acid (Sigma Chemical) for 5 min. Tests showed that polycarbonate filters were superior to the commonly used cellulose nitrate and cellulose acetate filters, as polycarbonate filters adsorb significantly less leucine, resulting in lower blanks and overall lower variability among replicate samples. The polycarbonate filters were placed in scintillation vials and stored at -20°C in the dark until the radioactivity of the filters was determined in the lab. One milliliter of ethylacetate was added, followed by 8 mL of scintillation cocktail (Insta-Gel Plus, Canberra Packard) after 10 min. The radioactivity incorporated into cells was counted in a liquid scintillation counter (LKB Wallac). Leucine incorporation rates were corrected for isotope dilution with added cold leucine and the ambient free L-leucine concentration was determined by HPLC. The leucine incorporation of the 0.8-μm-filtered seawater was converted to carbon production to calculate BGEs. A conservative theoretical conversion factor (CF) of 1.55 kg mol^{-1} Leu^{-1} C was used, disregarding internal isotope dilution (Kirchman 1993). To further constrain the BGEs, we also applied a CF of 3.1 kg mol^{-1} Leu^{-1} C assuming a twofold isotope dilution (Simon and Azam 1989) and the average of empirical CFs recently established for surface waters of the SATL (Alonso-Sáez et al. 2007).

Bacterial respiration—Bacterial respiration measurements followed the protocol described by Reinthaler et al. (2006). Briefly, the 0.8-μm filtrate was collected in a glass flask and subsequently dispensed to calibrated borosilicate glass biological oxygen demand (BOD) bottles with a nominal volume of 120 cm^3 using silicon tubing fixed to the spigot of the glass flask. For the determination of the initial O_2 concentration (t_0), samples were fixed immediately with Winkler reagents and incubated together with the live samples in water baths in the dark at in situ temperature ($\pm 1^\circ$C) for 12 h to 24 h, when the incubations were terminated (t_1). All the glassware was washed with 10% HCl and thoroughly rinsed with Milli-Q water before use. Oxygen concentrations of the t_0 and t_1 bottles were measured spectrophotometrically in a single run following the standard protocol for the determination of oxygen by Winkler titration. Measurements were done in a temperature-controlled laboratory container (set at 20°C) on a Technicon TRAACS 800 continuous-flow analysis system, connected to a custom-made autosampler (Reinthaler et al. 2006). The amount of total iodine was determined at a wavelength of 460 nm. The spectrophotometer was calibrated using standard additions of potassium iodate (J. T. Baker ACS grade KIO_3) to BOD bottles filled with seawater and adding Winkler chemicals in reverse order. The relative standard deviation calculated from triplicate samples was on average 0.08% at 220 μmol L^{-1} O_2. The oxygen consumption rates were converted to carbon units using a respiratory quotient of 0.89 (Williams and Del Giorgio 2005).

Calculations and statistics—The enrichment factors (EFs) for the individual parameters of the SML as compared with the ULW was calculated by dividing concentrations or rates determined for the SML by those for the ULW (EF = SML/ULW). Statistical analyses were performed with the software package STATISTICA from Statsoft.

Results

Physical properties—Along the transect in the SATL, salinity increased from the Mauritanian upwelling to the oligotrophic gyre from 36.1 to 37.7 (Fig. 2a) and surface water temperature from 25.8°C to 27.3°C (Fig. 2b). The wind speed measured around sampling at the individual stations was variable, ranging from 2 to 9.7 m s^{-1} (Fig. 2c). In the WMED, salinity was uniform with 38.0 ± 0.1 (Fig. 2d), as was surface temperature, averaging 24.8°C ± 0.3°C (Fig. 2e). Wind speed during sampling in the WMED varied between 2.8 and 8 m s^{-1} (Fig. 2f).

DOC, DON, DOP, and inorganic nutrient concentrations—The concentrations of DOC, DON, DOP, and inorganic nutrients measured at the different stations in the SML and the ULW are summarized in Table 2. In the SML, highest DOC concentrations were measured in the subtropical Atlantic shelf region under the influence of the Mauritanian upwelling system (439.2 μmol L^{-1}), gradually decreasing along the transect to ~110 μmol L^{-1} in the oligotrophic gyre. DOC concentrations in the ULW of the SATL were persistently lower than in the SML (by ~30%) and decreased from 344.7 to ~85 μmol L^{-1} along the transect (Table 2). In the SATL, DOC concentrations in the SML were positively related to the DOC concentrations in the ULW ($r^2 = 0.87$; $p < 0.0001$).

In the eddy system of the WMED, DOC concentrations in the SML were about twice as high as in the ULW, averaging 143.1 ± 25.3 μmol L^{-1} in the SML and 78.0 ± 10.8 μmol L^{-1} in the ULW (Table 2). Thus, at both study sites, the SML was significantly enriched in DOC as compared with the ULW, with enrichment factors ranging from 1.1 to 2.4 (Wilcoxon matched pairs test; $p = 0.005$, $n = 17$ and $p = 0.005$, $n = 10$ for the SATL and the WMED, respectively; Table 3).

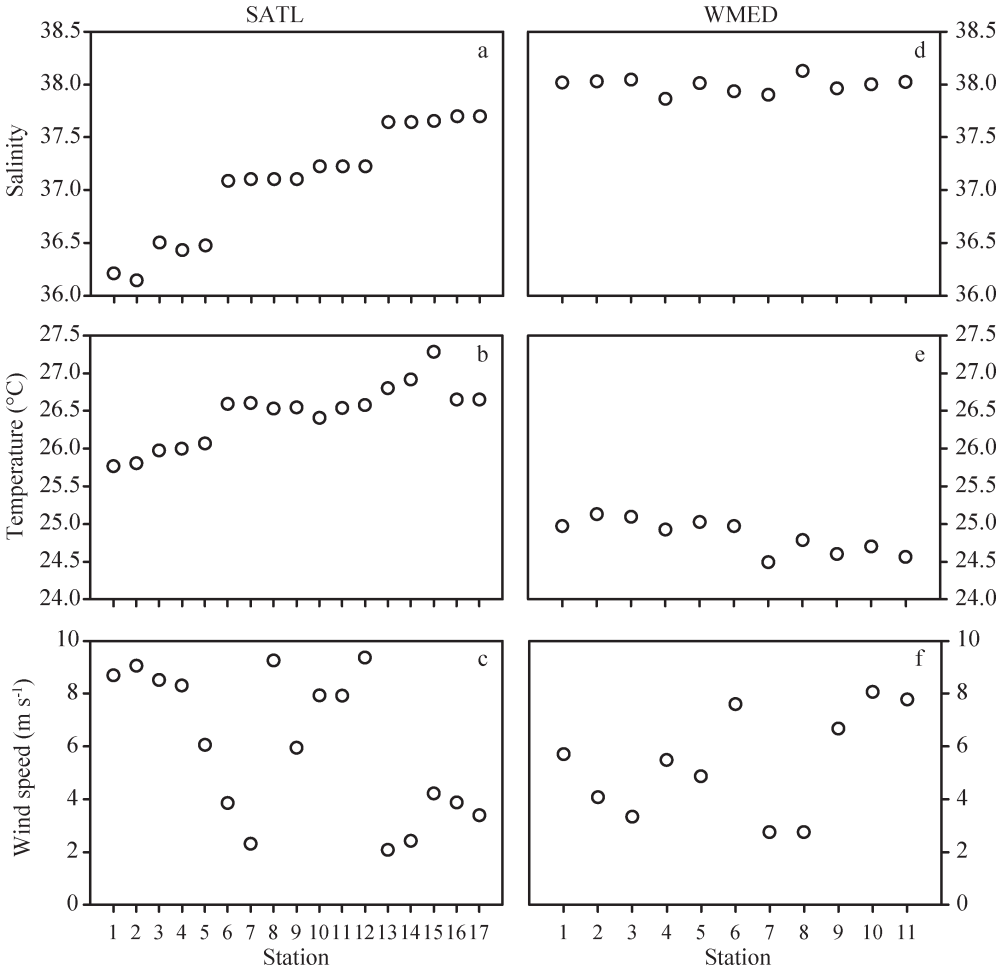

Fig. 2. Salinity, temperature (°C), and wind speed (m s^{-1}) at the different stations in (a, b, c) the subtropical Atlantic (SATL) and (d, e, f) the western Mediterranean (WMED).

To check for biases due to filtration, we also analyzed unfiltered total organic carbon (TOC) in WMED samples. TOC and DOC correlated very well ($y = -37.1 + 1.2x$, $r^2 = 0.93$, $p < 0.0001$, $n = 10$ and $y = 11.4 + 0.8x$, $r^2 = 0.89$, $p < 0.0001$, $n = 11$ for the SML and the ULW, respectively). On average, DOC concentrations were ~94% of the TOC in both the SML and ULW.

DON concentrations in the SML of the SATL were on average about three times higher than in the ULW (range in the SML: 7.9–37.4 μmol L^{-1}; Table 2). In the WMED, DON concentrations of the SML and ULW were similar to those obtained for the SATL (Table 2). Because of the higher enrichment in DON as compared with DOC in the SML at both sites (Table 3), the mean DOC : DON ratios for the SML (9.9 ± 7.5 for SATL, 8.1 ± 2.4 for WMED) were about half of the corresponding ratios for the ULW (Table 4). In contrast to DOC, no relationship was found between DON concentrations in the SML and the ULW at both study sites ($r^2 = 0.02$, $p = 0.6$ and $r^2 = 0.004$, $p = 0.8$ for the SATL and the WMED, respectively).

DOP concentrations are available only for the SATL. DOP concentrations decreased from the upwelling region to the oligotrophic gyre from 0.34 to 0.17 μmol L^{-1} in the SML and from 0.26 to 0.12 μmol L^{-1} in the ULW (Table 2). Thus, DOP was barely enriched in the SML as compared with the ULW, in contrast to DOC and particularly to DON (Table 3). As for DOC, a positive relationship was found between DOP concentrations in the SML and the ULW ($r^2 = 0.74$, $p < 0.0001$). The mean DOC : DOP ratio was similar in the SML and ULW; however, DON : DOP ratios were on average 78.3 ± 33.0 in the SML and thus significantly higher than the average DON : DOP ratio in the ULW (average: 28.9 ± 5.9, Mann–Whitney U-test; $p < 0.0001$), reflecting the enrichment in DON of the SML (Tables 3, 4).

At both study sites, inorganic nutrient concentrations in the ULW were generally low, reflecting open oceanic surface water conditions (Table 2). In the SML of the WMED, mean ammonium and nitrate concentrations were about one order of magnitude higher than in the corresponding ULW (Table 2). In the SML of the SATL, the mean ammonium concentration was one order of magnitude higher than in the ULW, whereas mean nitrate concentration was only about twice as high in the SML than in the ULW (Tables 2, 3). In the SATL and WMED, phosphate was enriched in the SML by a factor of two and

Table 2. Concentrations of DOC, DON, DOP, and inorganic nutrients (μmol L^{-1}) as well as the DIN : DIP measured at the different stations (STN) in the surface microlayer (SML) and the underlying water (ULW) of the SATL and the WMED. –, not measured.

	DOC		DON		DOP		NH_4		NO_3		NO_2		PO_4		DIN : DIP	
STN	SML	ULW	SML	ULW	SML	ULW	SML	ULW	SML	ULW	SML	ULW	SML	ULW	SML	ULW
								SATL								
1	439.2	344.7	11.8	6.0	0.34	0.26	2.050	0.155	0.190	0.050	0.036	0.022	0.152	0.108	15.0	2.1
2	370.5	208.5	37.4	6.2	0.33	0.31	3.733	0.136	0.440	0.000	0.044	0.010	0.212	0.102	19.9	1.4
3	186.3	158.1	19.7	6.5	0.28	0.25	0.917	0.175	0.200	0.050	0.017	0.011	0.182	0.157	6.2	1.5
4	207.6	88.7	30.0	6.4	0.28	0.23	3.272	0.233	0.120	0.040	0.026	0.012	0.437	0.192	7.8	1.5
5	142.8	88.8	12.8	5.7	0.23	0.23	1.050	0.155	0.090	0.020	0.014	0.011	0.166	0.148	7.0	1.3
6	110.0	81.4	13.3	5.5	0.23	0.23	1.876	0.185	0.034	0.028	0.017	0.012	0.044	0.043	43.8	5.2
7	121.1	86.8	14.6	5.8	0.27	0.19	2.055	0.289	0.024	0.035	0.018	0.013	0.044	0.028	47.7	12.0
8	121.1	81.9	14.9	5.3	0.24	0.20	0.694	0.188	0.078	0.070	0.017	0.019	0.038	0.018	20.8	15.4
9	102.0	82.2	12.8	5.6	0.24	0.21	0.802	0.194	0.039	0.020	0.015	0.013	0.036	0.022	23.8	10.3
10	98.3	79.2	13.5	5.0	0.23	0.18	0.143	0.573	0.029	0.205	0.013	0.012	0.011	0.031	16.8	25.5
11	116.2	87.8	13.5	5.6	0.22	0.21	1.452	0.265	0.046	0.047	0.018	0.013	0.036	0.025	42.1	13.0
12	174.4	82.2	21.6	4.9	0.22	0.17	2.196	0.193	0.049	0.004	0.015	0.012	0.036	0.021	62.8	10.0
13	110.6	82.1	11.6	6.3	0.20	0.14	1.076	0.242	0.020	0.043	0.010	0.009	0.025	0.008	44.2	36.8
14	97.7	80.8	24.0	5.0	0.21	0.15	4.047	0.201	0.103	0.008	0.011	0.009	0.052	0.009	80.0	24.2
15	95.6	83.3	24.2	4.6	0.22	0.15	1.515	0.175	0.042	0.004	0.009	0.010	0.043	0.008	36.4	23.6
16	115.8	85.5	7.9	4.5	0.14	0.13	0.542	0.275	0.027	0.220	0.007	0.009	0.022	0.012	26.2	42.0
17	131.4	87.9	27.0	4.7	0.17	0.12	2.482	0.175	0.016	0.019	0.010	0.006	0.020	0.007	125.4	28.6
Average	161.2	111.2	18.3	5.5	0.24	0.20	1.76	0.22	0.09	0.05	0.02	0.01	0.09	0.06	36.8	15.0
SD	98.0	69.2	7.9	0.7	0.05	0.05	1.13	0.10	0.11	0.06	0.01	0.00	0.11	0.06	30.6	13.0
								WMED								
1	152.4	82.1	19.6	7.1	–	–	4.097	0.510	0.526	0.060	0.025	0.009	0.029	0.018	160.3	32.2
2	138.4	69.7	17.1	3.5	–	–	3.806	0.133	0.711	0.002	0.032	0.012	0.034	0.014	133.8	10.5
3	124.6	82.4	17.4	4.5	–	–	2.674	0.220	0.368	0.036	0.013	0.005	0.019	0.012	160.8	21.8
4	150.2	73.3	18.8	3.7	–	–	2.969	0.141	0.371	0.032	0.020	0.004	0.042	0.010	80.0	17.7
5	129.5	75.6	17.5	6.0	–	–	1.750	0.371	0.520	0.003	0.022	0.006	0.044	0.021	52.1	18.1
6	118.7	73.6	16.6	3.9	–	–	1.278	0.134	0.387	0.010	0.022	0.008	0.024	0.011	70.3	13.8
7	157.4	105.5	11.0	5.1	–	–	1.046	0.250	0.362	0.107	0.040	0.014	0.035	0.019	41.4	19.5
8	–	–	18.5	5.6	–	–	1.331	0.181	0.280	0.026	0.024	0.007	0.051	0.015	32.1	14.3
9	103.0	67.0	11.1	4.3	–	–	1.402	0.161	0.214	0.003	0.024	0.006	0.033	0.017	49.7	10.0
10	170.0	74.0	27.2	4.4	–	–	2.798	0.125	0.289	0.003	0.025	0.010	0.075	0.011	41.5	12.5
11	187.0	77.0	31.5	4.2	–	–	2.136	0.139	0.261	0.001	0.019	0.008	0.071	0.012	34.0	12.3
Average	143.1	78.0	18.7	4.8	–	–	2.30	0.22	0.39	0.03	0.02	0.01	0.04	0.01	77.8	16.6
SD	25.3	10.8	6.0	1.1	–	–	1.05	0.12	0.14	0.03	0.01	0.00	0.02	0.00	50.0	6.4

three, respectively (Table 3). Dissolved inorganic nitrogen (DIN) concentrations showed no relationship between the SML and the ULW in the SATL and the WMED (r^2 = 0.09, p = 0.2 and r^2 = 0.09, p = 0.8, respectively). In the SATL, however, phosphate concentrations were positively correlated between the SML and ULW (r^2 = 0.91, $p < 0.0001$), whereas no such relationship was found for the WMED (r^2 = 0.01; p = 0.7). DIN to dissolved inorganic phosphorus (DIN : DIP) ratios in the ULW were close to Redfield (~16), whereas in the SML, mean DIN : DIP ratios were 36.8 ± 30.6 and 77.8 ± 50.0 in the SATL and WMED, respectively (Table 2).

Patterns in THAA, DFAA, and DCAA—In the SATL, the concentrations of THAA in the SML ranged from 1.1 to 25.8 μmol L^{-1} and in the ULW from 0.3 to 0.6 μmol L^{-1}, with no clear pattern along the transect (Table 5). In the SML, the contribution of DFAA to the THAA pool was remarkably high, averaging 47% ± 10%, whereas in the ULW, DFAA contributed only 12% ± 5% to the THAA pool (Mann−Whitney U-test; $p < 0.0001$; n = 17; Table 5).

THAA concentrations in the ULW were similar in the SATL and WMED and ranged between 0.3 and 1.0 μmol L^{-1} (Table 5). In the SML of the WMED, THAA concentrations varied within a narrow range from 2.8 to 5.3 μmol L^{-1}. The contribution of DFAA to the THAA was even higher in the WMED than in the SATL, averaging 61% ± 14% (Table 5). Remarkably, in the ULW of the WMED, the DFAA contribution to the THAA pool was three times higher than in the corresponding layer of the SATL (Table 5).

Composition of the dissolved THAA pool—Generally, the composition of the DFAA pool in the SML was similar to that of the ULW in both the SATL and the WMED, with L-serine, L-glycine, L-alanine, L-threonine/histidine, and L-aspartic acid together contributing 85.1% ± 2.5% and 78.5% ± 12.6% in the SML and the ULW of the SATL (Fig. 3a) and 85.9% ± 2.5% and 79.0% ± 3.8% in the SML and ULW of the WMED (Fig. 3c), respectively. However, the mole percentage distribution of individual amino acid species in the DCAA pool was significantly different (analysis of variance [ANOVA], $p < 0.05$) from that of

Table 3. Summary of enrichment factors (EF = SML/ULW) for selected chemical and biological parameters at the different stations (STN) in the subtropical Atlantic (SATL) and the western Mediterranean Sea (WMED). –, not measured or below detection limit.

STN	DOC	DON	DOP	NH_4	NO_3	NO_2	PO_4	DTAA	DFAA	DCAA	BA	Leu	BR
						SATL							
1	1.3	2.0	1.3	13.2	3.8	1.6	1.4	5.1	17.8	3.8	1.1	0.5	8.3
2	1.8	6.0	1.1	27.4	–	4.4	2.1	43.3	229.4	26.1	1.4	0.4	66.8
3	1.2	3.0	1.1	5.2	4.0	1.5	1.2	18.1	157.9	5.4	0.7	7.9	29.7
4	2.3	4.7	1.2	14.0	3.0	2.2	2.3	15.9	34.9	10.5	0.9	2.7	1.9
5	1.6	2.2	1.0	6.8	4.5	1.3	1.1	6.9	29.6	4.7	0.8	1.9	9.1
6	1.4	2.4	1.0	10.1	1.2	1.4	1.0	9.6	22.6	6.7	1.0	1.5	22.7
7	1.4	2.5	1.4	7.1	0.7	1.4	1.6	7.9	36.7	5.2	1.5	1.2	4.9
8	1.5	2.8	1.2	3.7	1.1	0.9	2.1	10.9	58.6	5.8	0.9	4.1	6.4
9	1.2	2.3	1.1	4.1	2.0	1.2	1.6	6.6	15.1	4.6	0.7	1.3	16.7
10	1.2	2.7	1.3	0.2	0.1	1.1	0.4	5.5	32.0	3.4	1.1	2.0	36.6
11	1.3	2.4	1.0	5.5	1.0	1.4	1.4	9.0	25.4	5.5	0.9	10.7	18.7
12	2.1	4.4	1.3	11.4	12.3	1.3	1.7	28.1	206.4	12.6	1.0	9.5	12.9
13	1.3	1.8	1.4	4.4	0.5	1.1	3.1	7.6	62.7	3.8	1.0	3.3	5.8
14	1.2	4.8	1.4	20.1	12.9	1.2	5.8	3.3	7.6	2.6	1.1	6.4	3.4
15	1.1	5.3	1.4	8.7	10.5	0.9	5.4	2.7	16.4	1.7	1.2	5.7	5.9
16	1.4	1.8	1.1	2.0	0.1	0.8	1.8	7.0	33.3	3.7	–	29.7	8.0
17	1.5	5.7	1.4	14.2	0.8	1.7	2.9	7.5	21.8	4.4	–	24.5	1.6
Average	1.5	3.3	1.2	9.3	3.7	1.5	2.2	11.5	59.3	6.5	1.0	6.7	15.3
SD	0.3	1.4	0.2	7.0	4.3	0.8	1.4	10.3	68.8	5.7	0.2	8.3	16.6
						WMED							
1	1.9	2.8	–	8.0	8.8	2.8	1.6	5.5	6.2	4.0	1.2	1.5	1.0
2	2.0	4.9	–	28.6	355.5	2.7	2.4	10.4	25.8	5.5	1.1	2.9	3.1
3	1.5	3.9	–	12.2	10.2	2.6	1.6	8.6	10.1	7.7	1.0	0.4	1.0
4	2.0	5.1	–	21.1	11.6	5.0	4.2	18.9	–	5.8	1.1	12.7	2.3
5	1.7	2.9	–	4.7	173.3	3.7	2.1	11.9	26.1	8.1	1.2	11.2	16.3
6	1.6	4.2	–	9.5	38.7	2.8	2.2	7.1	14.0	2.7	1.0	2.4	1.4
7	1.5	2.1	–	4.2	3.4	2.9	1.8	–	–	–	1.1	9.7	1.1
8	–	3.3	–	7.4	10.8	3.4	3.4	–	–	–	1.2	8.5	1.5
9	1.5	2.6	–	8.7	71.3	4.0	1.9	–	–	–	1.1	95.8	0.3
10	2.3	6.1	–	22.4	96.3	2.5	6.8	–	–	–	1.2	11.8	139.5
11	2.4	7.5	–	15.4	261.0	2.4	5.9	–	–	–	1.1	26.8	0.4
Average	1.8	4.1	–	12.9	94.6	3.1	3.1	10.4	16.5	5.6	1.1	16.7	15.3
SD	0.3	1.6	–	8.0	119.3	0.8	1.8	4.8	9.1	2.1	0.1	27.3	41.5

Table 4. DOC : DON, DOC : DOP, and DON : DOP ratios calculated for the different stations (STN) in the surface microlayer (SML) and the underlying water (ULW) of the SATL. DOC : DON ratios of the WMED are also shown. –, not measured.

	DOC : DON		DOC : DOP		DON : DOP		DOC : DON	
STN	SML	ULW	SML	ULW	SML	ULW	SML	ULW
				SATL				WMED
1	37.1	57.2	1,275.8	1,330.6	34.3	23.3	7.8	11.6
2	9.9	33.4	1,116.6	674.2	112.6	20.2	8.1	19.9
3	9.4	24.5	672.7	621.9	71.2	25.4	7.1	18.3
4	6.9	13.9	731.9	386.7	105.8	27.9	8.0	19.8
5	11.1	15.5	625.7	381.8	56.1	24.7	7.4	12.7
6	8.3	14.7	482.4	350.4	58.4	23.8	7.2	18.8
7	8.3	15.0	450.7	449.9	54.4	29.9	14.3	20.6
8	8.1	15.3	502.9	403.7	61.8	26.4	0.0	0.0
9	8.0	14.6	432.2	386.5	54.1	26.5	9.3	15.8
10	7.3	15.9	432.5	450.3	59.3	28.3	6.3	16.7
11	8.6	15.7	530.7	412.3	61.8	26.2	5.9	18.3
12	8.1	16.8	784.4	485.2	97.2	28.8	–	–
13	9.5	13.1	554.8	566.6	58.3	43.4	–	–
14	4.1	16.2	473.7	535.9	116.4	33.1	–	–
15	4.0	18.2	437.2	549.0	110.5	30.2	–	–
16	14.6	19.2	840.9	654.0	57.6	34.1	–	–
17	4.9	18.5	786.9	739.9	161.5	39.9	–	–
Average	9.9	19.9	654.8	551.7	78.3	28.9	8.1	17.2
SD	7.5	10.8	246.7	232.3	33.0	5.9	2.4	3.1

Table 5. Concentrations of dissolved total hydrolysable amino acids (THAA; μmol L^{-1}), dissolved free amino acids (DFAA; μmol L^{-1}), dissolved combined amino acids (DCAA; μmol L^{-1}), and the percentage of DFAA to the THAA pool measured at the different stations (STN) in the subtropical Atlantic (SATL) and the western Mediterranean Sea (WMED). –, below detection limit.

	THAA (μmol L^{-1})		DFAA (μmol L^{-1})		DCAA (μmol L^{-1})		DFAA:THAA (%)	
STN	SML	ULW	SML	ULW	SML	ULW	SML	ULW
				SATL				
1	2.70	0.53	0.87	0.05	1.83	0.48	32	9
2	25.82	0.60	11.58	0.05	14.25	0.55	45	8
3	8.14	0.45	5.90	0.04	2.23	0.41	73	8
4	9.02	0.57	4.37	0.13	4.65	0.44	48	22
5	3.29	0.48	1.27	0.04	2.02	0.43	39	9
6	3.97	0.42	1.68	0.07	2.29	0.34	42	18
7	3.17	0.40	1.27	0.03	1.90	0.37	40	9
8	5.01	0.46	2.59	0.04	2.41	0.42	52	10
9	3.39	0.51	1.48	0.10	1.91	0.42	44	19
10	2.11	0.38	0.88	0.03	1.23	0.36	42	7
11	4.55	0.51	2.27	0.09	2.29	0.42	50	18
12	10.86	0.39	6.38	0.03	4.47	0.36	59	8
13	2.58	0.34	1.36	0.02	1.23	0.32	53	6
14	1.36	0.41	0.43	0.06	0.93	0.35	31	14
15	1.14	0.42	0.46	0.03	0.68	0.39	40	7
16	2.72	0.39	1.43	0.04	1.30	0.35	52	11
17	2.87	0.38	1.47	0.07	1.40	0.32	51	18
Average	5.45	0.45	2.69	0.05	2.77	0.39	47	12
SD	5.91	0.07	2.89	0.03	3.15	0.06	10	5
				WMED				
1	5.26	0.96	3.76	0.60	1.55	0.39	71	63
2	3.37	0.32	1.89	0.07	1.51	0.27	56	23
3	4.80	0.56	2.11	0.21	2.72	0.35	44	37
4	4.92	0.26	3.42	–	1.52	0.26	70	–
5	5.08	0.43	2.38	0.09	2.71	0.33	47	21
6	2.82	0.40	2.19	0.16	0.64	0.24	78	39
Average	4.37	0.49	2.63	0.23	1.78	0.31	61	37
SD	1.02	0.25	0.77	0.22	0.80	0.06	14	17

the DFAA pool. L-Glycine and L-glutamic acid contributed 53.8% ± 9.2% to the DCAA pool in the SML and 43.6% ± 2.6% in the ULW of the SATL (Fig. 3b). The mole percentage distribution in the WMED was similar to that of the SATL, albeit the contribution of L-glycine and L-glutamic acid to the DCAA pool was slightly higher in the WMED, averaging 71.3% ± 14.6% in the SML and 52.6% ± 10.3% in the ULW, respectively (Fig. 3d). At both sites, L-glutamic acid contributed about three times more to the DCAA pool of the SML than in the ULW (Fig. 3b, d). Thus, at both sites, the composition of the DCAA pool in the SML did not resemble its composition in the ULW as closely as the DFAA pool. No relationship of individual amino acid mole percentages or pooled dissolved amino acid concentrations was found between the SML and ULW. D-Enantiomeric amino acids generally contributed <3% to the THAA pool.

At both study sites, mean concentrations of individual DFAA species in the SML ranged from 6 nmol L^{-1} to 874 nmol L^{-1} (see Web Appendix 1 at www.aslo.org/lo/toc/vol_53/issue_1/0122a1.pdf). The DFAA concentrations in the ULW were generally significantly lower than in the SML, ranging from ~1 to 27 nmol L^{-1} (data from both sites pooled, ANOVA, $p < 0.05$). In the SML of the SATL, concentrations of individual amino acids of the DFAA pool were not significantly different from concentrations measured in the SML of the WMED (ANOVA, $p = 0.2$), whereas in the ULW, some DFAA species were slightly higher in the WMED than in the SATL. At both study sites, the mean concentrations of individual amino acids of the DCAA pool ranged from ~19 to 744 nmol L^{-1} in the SML and from ~3 to 131 nmol L^{-1} in the ULW (see Web Appendix 1). As for the DFAA pool, concentrations of individual amino acids in the DCAA pool of the ULW were significantly lower than in the SML (ANOVA, $p < 0.05$).

Changes in the amino acid composition as indicator of organic matter diagenesis—To characterize the changes in the amino acid pool along the transect in the SATL, a principal component analysis (PCA) was used on the basis of a matrix of mole percentages of the different THAA in the SML and ULW (Fig. 4a, b). The site scores along axis 1 indicate the relative degradation state of the THAA pool, with more negative site scores representing more decomposed material and more positive scores reflecting more freshly produced dissolved organic matter (DOM) (Dauwe et al. 1999). Using this approach, we obtained a rather variable pattern in the SML of the SATL, indicating a complex production and degradation pattern

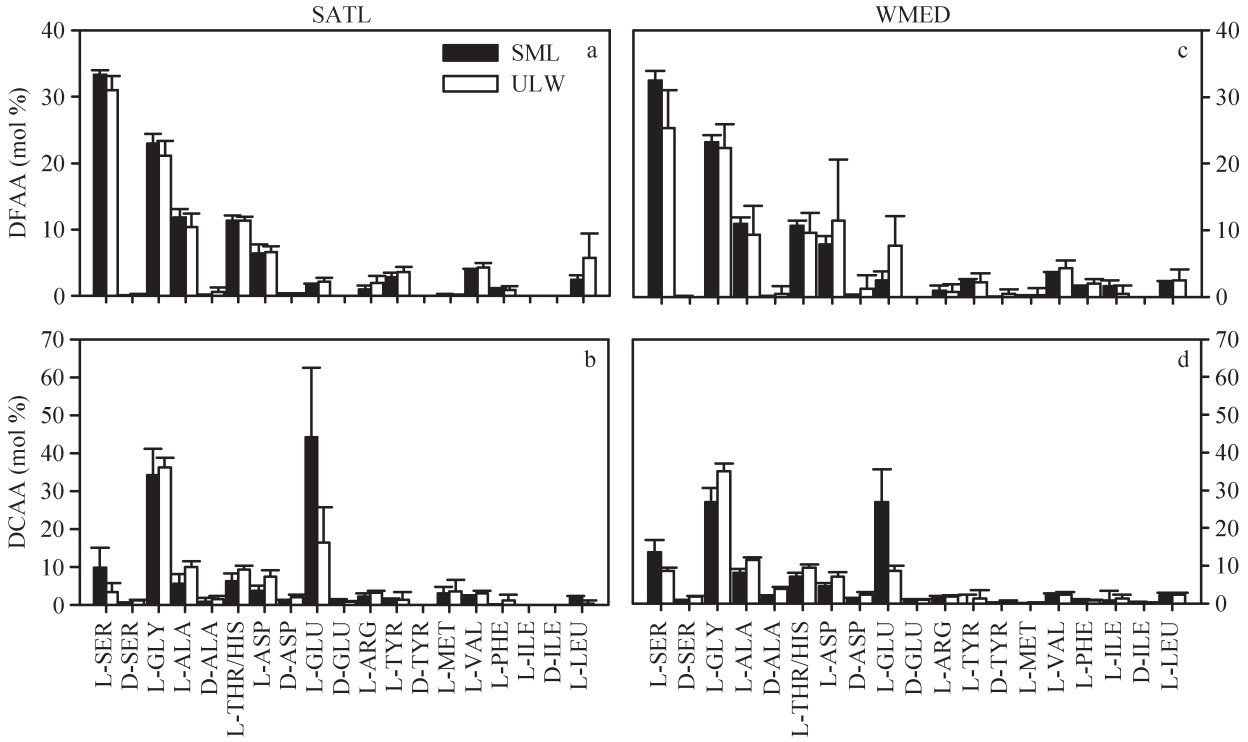

Fig. 3. Average mole percentages of the L- and D-amino acids of the DFAA and the DCAA pool in the surface microlayer (SML) and underlying water (ULW) of (a, b) the subtropical Atlantic (SATL) and (c, d) the western Mediterranean (WMED). Error bars denote standard deviations.

of amino acids in the SML (Fig. 4a). In the ULW, however, the DOM pool became progressively more refractory and degraded along the transect from the upwelling area to the oligotrophic gyre (Fig. 4b). Further evidence for increasing degradation of the THAA pool toward the oligotrophic gyre is derived from the increase in the D : L ratios of alanine and aspartic acid (Fig. 4c, d). This increase in the D : L ratios of alanine and aspartic acid was more pronounced in the ULW than in the SML (Fig. 4c, d). No changes in the D : L ratio for glutamic acid were detected, however, along the transect in SATL. The low number of amino acid data from the WMED precluded a similar analysis as described above for SATL.

Bacterial abundance—In the SATL, bacterial abundance in the SML and the ULW decreased by a factor of four from the upwelling region to the SATL gyre (Fig. 5a) with no apparent enrichment in the SML (Wilcoxon matched pairs test, $p = 0.9$, $n = 15$, Table 3). Bacterial abundance in the SML was positively related to that in the ULW ($r^2 = 0.67$, $p < 0.001$).

Bacterial abundance in the WMED did not exhibit a specific trend over time (Fig. 5d). Mean bacterial abundance was $6.8 \pm 0.5 \times 10^8$ cells L^{-1} in the SML and $6.1 \pm 0.3 \times 10^8$ cells L^{-1} in the ULW. Bacterial abundance in the SML of the WMED was enriched by a factor of 1.1 $\pm$ 0.1 (Wilcoxon matched pairs test, $p = 0.003$, $n = 11$, Table 3). As for the SATL, bacterial abundance between SML and ULW was positively related in the WMED ($r^2 = 0.56$; $p < 0.01$).

Leucine incorporation rates—In the SATL, leucine incorporation in the SML was variable, ranging from 3 to 50 pmol L^{-1} h^{-1} (Fig. 5b). In the ULW of the SATL, leucine incorporation declined from the highly productive upwelling region (~20 pmol L^{-1} h^{-1}) to the gyre (3 pmol L^{-1} h^{-1}; Fig. 5b). In the upwelling region, leucine incorporation in the SML was about half of that in the ULW (Table 3). In the gyre of the SATL, however, bacterial leucine incorporation rates were higher, with enrichment factors ranging from 1.2 to 30 (Table 3).

In the SML of the WMED, leucine incorporation varied over two orders of magnitude, ranging from 7 to 488 pmol L^{-1} h^{-1}, whereas in the ULW, leucine incorporation was lower, ranging from 5 to 38 pmol L^{-1} h^{-1} (Fig. 5e). Thus, leucine incorporation in the SML and ULW of the WMED was on average higher than in the corresponding layers of the SATL. Leucine incorporation rates in the SML of the WMED were highly variable and enrichment factors ranged from 0.4 to 96 (Table 3). In both SATL and WMED, leucine incorporation rates in the SML and ULW were not related to each other ($r^2 = 0.11$, $p = 0.2$ and $r^2 = 0.12$, $p = 0.3$ for the SATL and the WMED, respectively). Leucine incorporation measured in unfiltered and 0.8-μm-filtered seawater was highly correlated in both the SML and the ULW (Spearman rank correlation, $r = 0.95$, $p <$

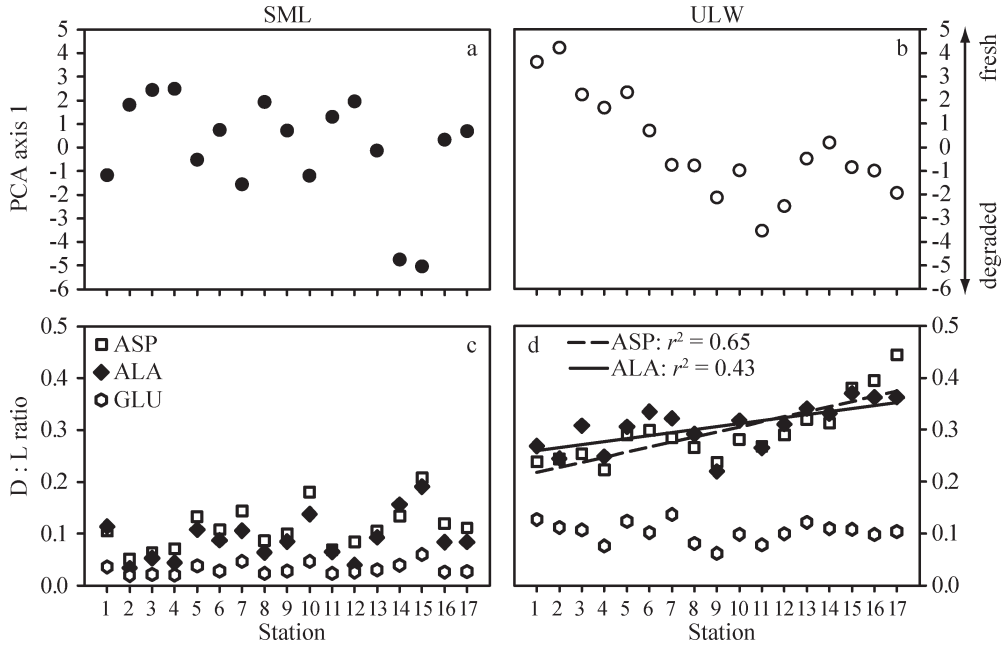

Fig. 4. Diagenesis of the amino acid pool in the surface microlayer (SML) of the subtropical Atlantic. The degradation index (PCA axis 1) is based on a principal component analysis of the mole percentages of the individual amino acids in the dissolved total dissolved amino acid pool (THAA). High scores indicate more freshly produced amino acids, whereas low scores are an indication of a relatively degraded amino acid pool in (a) the SML and (b) the ULW. D : L amino acid ratios for aspartic acid (ASP), alanine (ALA), and glutamic acid (GLU) in the (c) surface microlayer (SML) and (d) underlying water (ULW) of the subtropical Atlantic.

0.01). On average, leucine incorporation rates in 0.8-μm-filtered seawater were 5–30% lower compared with that in unfiltered seawater.

Bacterial respiration—In the SML of the SATL, bacterial respiration was high in the upwelling region (9.5 $\pm$ 0.9 μmol L^{-1} d^{-1} O_2) and decreased toward the oligotrophic gyre (3.6 $\pm$ 2.0 μmol L^{-1} d^{-1} O_2), although at two gyre stations high respiration rates were recorded as well (Fig. 5c). In contrast, bacterial respiration in the ULW was consistently low (0.8 $\pm$ 0.8 μmol L^{-1} d^{-1} O_2) along the transect (Fig. 5e). Thus, bacterial respiration was significantly higher in the SML than in the ULW (Wilcoxon matched pairs test, $p = 0.0003$, $n = 17$), with enrichment factors ranging from 1.6 to 67. Generally, lower enrichment factors were found in the oligotrophic gyre region than in the upwelling region (Table 3).

In the WMED, bacterial respiration was highly variable between the different stations in both the SML and ULW (Fig. 5f). Comparing average bacterial respiration rates between the two study sites for the SML and ULW separately, no significant difference was found (Student's *t*-test, $p = 0.2$ and $p = 0.1$ for the SML and ULW, respectively). As for bacterial leucine incorporation, bacterial respiration in the SML was not related to that in the ULW at both sites ($r^2 = 0.45$, $p = 0.07$ and $r^2 = 0.23$, $p = 0.13$ for SATL and WMED, respectively).

Bacterial growth efficiencies (BGEs)—BGE (BGE = bacterial carbon production [BP]/[BP + bacterial carbon respired {BR}]) was calculated from leucine incorporation rates using 1.55 kg C mol^{-1} Leu incorporated to calculate BP and bacterial oxygen consumption was converted to BR using a respiratory quotient of 0.89. At the SATL transect, BGE was low and on average 0.7% $\pm$ 0.2% in the SML and 4.1% $\pm$ 1.8% in the ULW (Table 6). In the WMED, BGE was on average 8.5% $\pm$ 3.8% in the SML and 8.9% $\pm$ 3.4% in the ULW (Table 6). In the SATL and the WMED average BGEs were not significantly different between the SML and ULW (Student's *t*-test, $p = 0.07$ and $p = 0.9$ for the SATL and the WMED, respectively). To constrain the BGE, we also used two other CFs, one commonly used (Simon and Azam 1989) and one recently determined for the subtropical surface waters of the North Atlantic (Alonso-Sáez et al. 2007). As shown in Table 6, the recently determined CF results in about seven-times-lower BGEs than using the CF without isotope dilution taken into account (1.55 kg C mol^{-1} Leu incorporated).

Discussion

Evaluation of potential problems associated with the methods used—It is well documented that the sampling efficiency of the SML varies depending on the biological and chemical components examined and on the sampling device used. Although the commonly used metal screen sampler (Garrett 1967) allows for relatively rapid sampling of up to 100 mL per dip, the resulting SML sample is usually diluted with ULW (Hatcher and Parker 1974). Recently it was found, however, that a glass plate sampler

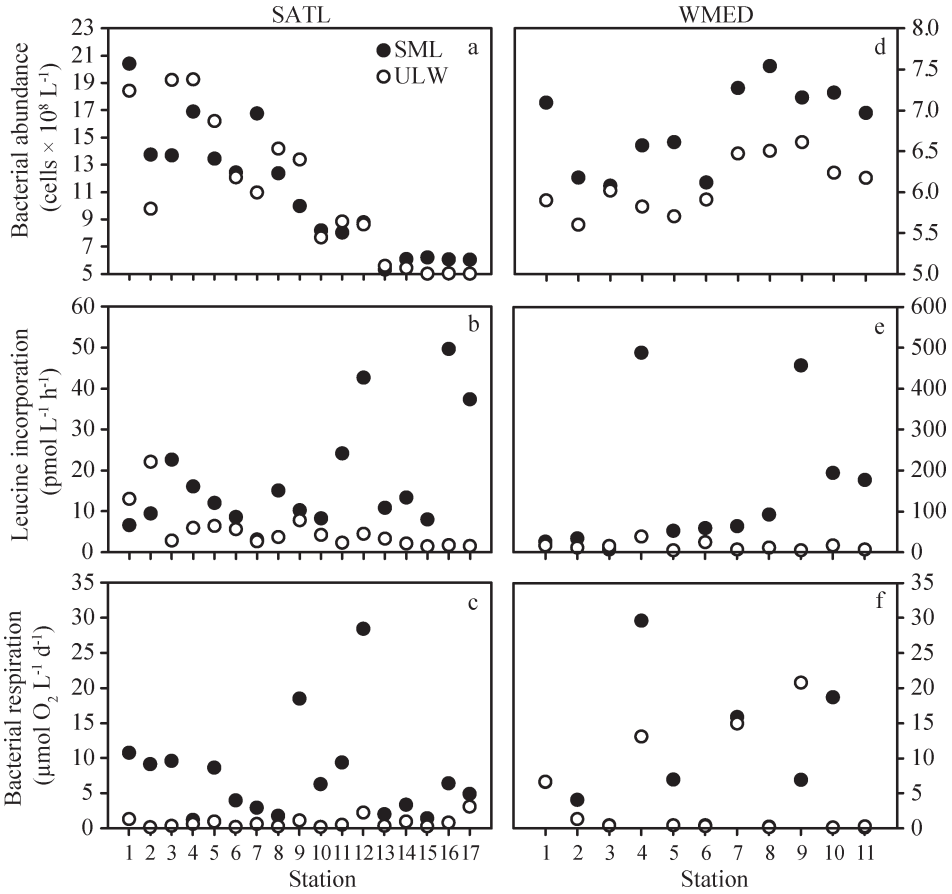

Fig. 5. Bacterial abundance (cells $\times$ 10^8 L^{-1}), leucine incorporation (pmol L^{-1} h^{-1}), and respiration (μmol L^{-1} d^{-1} O_2) measured in the surface microlayer (SML) and the underlying water (ULW) at the different stations in (a, b, c) the subtropical Atlantic (SATL) and (d, e, f) the western Mediterranean eddy (WMED).

(Harvey and Burzell 1972) is the better choice for studies of inorganic and organic nutrients (Momzikoff et al. 2004) and for bacteria (Agogué et al. 2004).

Diel variations of DOC concentrations and bacterial activity in the euphotic zone have been reported for the Mediterranean Sea (Gasol et al. 1998) and for bacterial abundance also in the SATL (Kuipers et al. 2000). Thus, whenever possible, we sampled in the morning, at noon, and in the late afternoon. No clear diel patterns in the chemical properties or bacterial activity were detected, however, either in the SML or in the ULW. High variations in physicochemical parameters on smaller temporal scales seem to be typical for the SML (Kuznetsova and Lee 2002 and references therein). Additionally, the variable influence of the wind during the sampling period presumably masks diel patterns in the top centimeter layers of the open ocean.

The requirement to perform the biological rate measurements in incubation flasks alters the originally high-surface low-volume habitat of the surface microlayer and disrupts the interactions of the SML with the ULW and the atmosphere. Thus, the property changes of specific physical and chemical parameters might lead to altered bacterial activity measurements as compared with the actual in situ rates. In an attempt to minimize these effects, the incubations of SML samples were run as short as possible, i.e., ~0.5 h for bacterial production and ~14 h for respiration measurements. Albeit these inherent problems, however, bacterial respiration and bacterial production are

Table 6. Mean ± SE in parentheses of bacterial growth efficiencies in the SATL and the WMED calculated with different conversion factors (CF) to convert leucine incorporation into bacterial carbon production. (A) Theoretical CF assuming no isotope dilution (1.55 kg C mol^{-1} Leu) (Kirchman 1993), (B) average of empirical CFs from open-ocean stations in SATL (0.18 kg C mol^{-1} Leu) (Alonso-Sáez et al. 2007), and (C) theoretical CF assuming twofold internal isotope dilution (Simon and Azam 1989). *n* denotes the number of stations for which the bacterial growth efficiency was determined.

			Bacterial growth efficiency (%)		
Region	Depth	*n*	A	B	C
SATL	SML	17	0.7 (0.2)	0.1 (0.02)	1.3 (0.4)
	UWL	17	4.1 (1.8)	0.6 (0.3)	7.2 (2.8)
WMED	SML	11	8.5 (3.8)	1.3 (0.7)	13.8 (5.5)
	UWL	11	8.9 (3.4)	1.3 (0.5)	14.7 (5.2)

probably affected similarly because of confinement and therefore their relation to each other is probably not substantially altered.

To the best of our knowledge, direct bacterial respiration measurements from the open-ocean surface microlayer are not available. Bacterial respiration in the SATL and the WMED varied over a wide range, from ~0.1 to 30 μmol O_2 L^{-1} d^{-1}, and was occasionally exceptionally high. However, the bacterial respiration rates we measured in the euphotic zone for the SATL (0.6 ± 0.5 μmol O_2 L^{-1} d^{-1}, n = 66) and the WMED (0.3 ± 0.2 μmol O_2 L^{-1} d^{-1}, n = 71) were comparable with other open-ocean sites (Lemée et al. 2002; González et al. 2003). Further support for the quality of our respiration data comes from measurements of total community respiration of unfiltered seawater in the SATL. Bacterial respiration and total community respiration in the SATL were highly related (r^2 = 0.84, $p < 0.001$, n = 17 and r^2 = 0.59, $p < 0.01$, n = 15, data not shown), which suggests that we were able to track the generally increasing influence of microbial activity from the upwelling toward the subtropical gyre. Furthermore, high respiration rates in the SML are indicated by a study in the SATL measuring CO_2 supersaturation in the top centimeter layer (Calleja et al. 2005).

Our leucine incorporation rates in the SML were on average at the lower end compared with rates from the euphotic zone of the same area (Van Wambeke et al. 2004, Alonso-Sáez et al. 2007). Leucine uptake measurements are usually conducted with the assumption that the concentrations of free amino acids are rather low; however, the free leucine concentrations in the SML and ULW at both study sites were highly variable and ranged from 1 to 244 nmol L^{-1} (see Web Appendix 1). Variable free leucine concentrations in the ambient water leads to varying external isotope dilution. Hence, we included the concentration of ambient free leucine in the calculations of bacterial leucine incorporation.

Experiments to empirically determine factors to convert bacterial leucine incorporation rates into carbon biomass production were not performed in this study; instead, a range of CFs was used to constrain BGEs (Table 6). The BGEs in the SML were <14%, suggesting that most of the DOC taken up was used for cell maintenance rather than growth (Del Giorgio and Cole 2000). The only other reported BGEs for the surface microlayer are from the coastal French Mediterranean Sea and range from 18% to 83% (Obernosterer et al. 2005). The latter values were calculated using the average of the bacterial production measured at time zero and after 24 h. Following this approach for samples from the SATL where we have the required data, we arrive at a BGE of 56% ± 20% for the SML (n = 12) and 14% ± 12% for the ULW (n = 10). However, the relationship between bacterial production measured in unfiltered and 0.8-μm-filtered seawater was weak after 12–18 h. Respiration measurements integrate over longer timescales (~12–24 h) than bacterial production measurements (~0.5–1 h) and it has been shown that despite increased growth in incubations, oxygen concentrations in the BOD bottles decline linearly (Alonso-Sáez et al. 2007). The latter indicates that longer incubation times do not necessarily affect respiration rates. However, the development of respiration rates in confinement remains controversial and more work is needed to resolve this issue (Pomeroy et al. 1994; Briand et al. 2004).

For the WMED, bacterial production was measured only at initial time points. However, for a few samples of the SML and UWL we followed the abundance of bacterial cells over the duration of the incubations to calculate bacterial production from the increase in cell abundance. Applying a mean carbon content of 15 fg C $cell^{-1}$ (Fukuda et al. 1998), we arrive at a BGE of 37% ± 42% and 58% ± 37% for the SML and ULW, respectively.

Mean BGEs calculated with these alternative methods seem high compared with BGEs on the basis of time zero bacterial production measurements reported for the euphotic layer of the open ocean ranging from ~15% to 20% (Del Giorgio and Cole 2000). Moreover, such high BGEs would indicate that the available substrate is efficiently utilized, which is apparently not the case, on the basis of the enrichment of the potential nitrogen sources. Particularly the bacteria in the SML are not utilizing the DFAA pool efficiently, as indicated by the high contribution of DFAA to the THAA pool (Table 5).

Accumulation of DOM in the SML—DOC concentrations at 10-m depth were 74.7 ± 6.9 μmol L^{-1} and 83.2 ± 8.4 μmol L^{-1} in the SATL and the WMED, respectively. Other studies performed in these areas report DOC concentrations ranging from 50 to 90 μmol L^{-1} (Dafner et al. 1999; Santinelli et al. 2002). The higher DOC concentrations in the SML and ULW, however, agree with earlier studies reporting increased DOC concentrations for the ULW and enrichment factors of 1.5–1.8 (Williams et al. 1986). It has been shown that ultraviolet (UV) radiation renders initially labile organic matter more refractory and vice versa (Obernosterer et al. 1999). UV radiation is inhibiting bacterial activity (Herndl et al. 1993) and it is likely that the bacterioplankton in the SML receives a high dose of solar radiation. Therefore, a scenario of inhibited bacterioneuston activity and abiotically produced refractory DOC could explain at least some of the accumulation in the SML. However, whether the formation of refractory DOM from more labile organic matter prevails over the photochemical production of labile DOM in the SML remains to be shown.

For efficient bacterial assimilation of DOM, its elemental composition should match the C : N : P ratio of bacteria of about 50 : 10 : 1 (Goldman et al. 1987). In the SML and ULW at both study sites about 90% of the total nitrogen was present as DON. This is at the high end of reported DON contributions to the total dissolved nitrogen pool in the ocean (Bronk 2002). The fraction of DOP of the total dissolved phosphorus pool (~80%), however, was similar to other studies (Karl and Björkman 2002). The DOM in the ULW was relatively depleted in DON (C : N = 18.2 ± 9.3; average of SATL and WMED), whereas the DOM of the SML was nitrogen rich (C : N = 8.9 ± 6.2; average of SATL and WMED). For comparison, DOC : DON ratios range between 8 and 16 in the euphotic waters of the North Atlantic and the NW Mediterranean Sea (Kähler and

Koeve 2001; Aminot and Kérouel 2004). The higher DON concentration in the SML might originate from atmospheric input or selective scavenging of nitrogenous compounds from the ULW (Béthoux and Copin-Montégut 1986; Vidal et al. 1999). The C : N ratios in the ULW of the SATL were variable, with a tendency of higher ratios in the upwelling and decreasing ratios toward the gyre (Table 3). This may reflect the generally higher productivity in upwelling systems with accompanied excess DOC production by rapidly growing phytoplankton (Teira et al. 2001). In contrast, the subtropical gyre is a major site of N_2 fixation by *Trichodesmium* (Capone et al. 1997). Hence relatively more DON than DOC might be released here than in the upwelling region (Vidal et al. 1999). The potential importance of N_2-fixing prokaryotes in the gyre system is supported by relatively stable ammonium concentrations from the upwelling area toward the gyre, whereas nitrate and phosphate concentrations declined by at least one order of magnitude along the transect (Table 2).

It has been shown experimentally that increasing C : N ratios of the DOM pool leads to decreasing bacterial growth efficiencies because bacteria have to respire relatively more carbon to cover their nitrogen demand (Goldman et al. 1987; Kroer 1993). Accordingly, one would expect that BGEs are higher in the SML than in the ULW, considering the relatively nitrogen-rich DOM in the SML. However, BGEs in the SML were not significantly different from those in the ULW. In the SATL, DON : DOP ratios for the ULW were lower than reported for the surface ocean, while those of the SML were substantially higher, indicating selective accumulation of DON in the SML (Vidal et al. 1999; Aminot and Kérouel 2004). Simple relationships between the nutrient ratios and BGEs were not found in the present study, confirming that the bulk C : N in natural environments might be a weak indicator for the actual substrate source for bacteria (Del Georgio and Cole 2000). DFAA usually cover a considerable fraction of the bacterial nitrogen demand and exhibit high turnover rates (Suttle et al. 1991). In the SML, DFAA are highly enriched as compared with the concentrations in the ULW (Table 5), as also reported elsewhere (Kuznetsova et al. 2004). At both study sites, THAA contributed, in terms of carbon, ~12% to the DOC pool in the SML and ~2% in the ULW. Likewise, the amino acid yield was 30% and 14% of the DON pool of the SML and ULW, respectively. This suggests that THAA constitute an important fraction of the DOC and DON pool in the SML. DFAA comprised 47–61% of the THAA in the SML (Table 5). In the ULW, the contribution of DFAA to the THAA pool was significantly lower (12–37%). Kuznetsova and Lee (2002), finding similarly high contributions of DFAA to the THAA pool, hypothesized that the hydrolysis of DCAA may predominately produce short peptides that are potentially taken up faster than DFAA. Alternatively, the authors also speculated that the physiological state of SML bacteria might be different from that in the ULW, leading to the enrichment in DFAA in the SML. In the coastal Mediterranean Sea, however, phylogenetic analysis of the bacterial community of the SML did not reveal major differences from that in the ULW (Agogué et al. 2005). This apparent phylogenetic similarity of the bacterial communities in the SML and ULW does not preclude, however, subtle physiological differences between the communities.

The turnover time of leucine (concentration of dissolved free leucine : leucine uptake by bacteria) in the SML ranges from 0.1 to 24 h and from 0.1 to 2 h in the ULW. Fuhrman (1987) calculated amino acid turnover times ranging from 0.2 to 2.4 h and Suttle et al. (1991) report for Sargasso Sea surface waters a leucine turnover time of ~22 h. Thus, despite our similar leucine turnover time the exceptionally high contribution of DFAA to the THAA pool suggests a major decoupling of DFAA production and bacterial DFAA uptake. One explanation for the decoupling might be that the release of DFAA by autotrophs inhabiting the SML is elevated because of UV stress (Pausz and Herndl 1999), while the prokaryotic uptake of substrate is reduced under UV stress (Herndl et al. 1993). However, we did not observe diel variations in the DFAA concentrations, the contribution of DFAA to the THAA pool, and bacterial leucine incorporation and respiration. This indicates that UV radiation is either not a major factor controlling DFAA utilization in the SML or that UV-mediated bacterial inhibition is compensated for by the photochemical production of DOM readily available to the SML bacterial community.

Changes in the THAA composition have been used as indicator of organic matter diagenesis (Dauwe et al. 1999). DCAA adsorb more efficiently to particles than DFAA (Kuznetsova and Lee 2002) and therefore might not be readily available for bacterioplankton. Using this approach, a gradual aging of the DOM pool from the upwelling area toward the subtropical gyre in the ULW of the SATL was apparent (Fig 4b). Moreover, the increasing D : L ratio of the amino acid pool from the upwelling area to the gyre also indicates a diagenetic alteration of the DOM pool (Amon et al. 2001). The gradually increasing D : L ratio of aspartic acid and alanine in the ULW suggests preferential utilization of L-amino acids (Pérez et al. 2003) and generally, a tendency toward lower bioreactivity of the DOM from the upwelling area toward the oligotrophic gyre in the ULW (Fig. 4d). The lack of any trend in the amino acid composition and the D : L amino acid ratios in the SML along the transect from the upwelling system to the oligotrophic gyre, however, suggests that the DOM pool of the SML is regularly replenished. The renewal of the DOM in the SML is most likely only to a minor extent mediated by the ULW because similar patterns in the D : L amino acid ratios and the amino acid composition would be expected then. This suggests that replenishment of the DOM pool of the SML is probably largely mediated by autochthonous DOM production.

In conclusion, we found that the SML in the open ocean is a highly variable environment with high concentrations of DFAA and a high contribution of the THAA to the DON pool. Despite the mean DFAA concentration in the SML being one order of magnitude higher than in the ULW, the BGEs are similar in the SML and the ULW. The generally low BGEs strongly indicate that the DFAA in the

SML are not readily available for bacteria. Bacterial respiration in the SML is high, supporting the idea of biological control of CO_2 fluxes across the air–sea interface. The role of UV radiation on DOM and the microbiota of the SML and the reasons for the accumulation of DFAA in the SML deserve further investigation.

References

Agogué, H., F. Joux, I. Obernosterer, and P. Lebaron. 2005. Resistance of marine bacterioneuston to solar radiation. Appl. Environ. Microbiol. **71:** 5282–5289.

———, and others. 2004. Comparison of samplers for the biological characterization of the sea surface microlayer. Limnol. Oceanogr. Methods **2:** 213–225.

Alonso-Sáez, L., J. M. Gasol, J. Arístegui, J. C. Vilas, D. Vaqué, C. M. Duarte, and S. Agustí. 2007. Large-scale variability in surface bacterial carbon demand and growth efficiency in the subtropical North East Atlantic Ocean. Limnol. Oceanogr. **52:** 533–546.

Aminot, A., and R. Kérouel. 2004. Dissolved organic carbon, nitrogen and phosphorus in the North East Atlantic and the North West Mediterranean with particular reference to non-refractory fractions and degradation. Deep-Sea Res. I **51:** 1975–1999.

Amon, R. M. W., H.-P. Fitznar, and R. Benner. 2001. Linkages among the bioreactivity, chemical composition, and diagenetic state of marine dissolved organic matter. Limnol. Oceanogr. **46:** 287–297.

Béthoux, J. P., and G. Copin-Montégut. 1986. Biological fixation of atmospheric nitrogen in the Mediterranean Sea. Limnol. Oceanogr. **31:** 1353–1358.

Briand, E., O. Pringault, S. Jacquet, and J.-P. Torréton. 2004. The use of oxygen microprobes to measure bacterial respiration for determining bacterioplankton growth efficiency. Limnol. Oceanogr. Methods **2:** 406–416.

Bronk, D. A. 2002. Dynamics of DON, p. 153–247. *In* D. A. Hansell and C. A. Carlson [eds.], Biogeochemistry of marine dissolved organic matter. Academic Press.

Calleja, M. L., C. M. Duarte, N. Navarro, and S. Agustí. 2005. Control of air–sea CO_2 disequilibria in the subtropical North East Atlantic by planktonic metabolism under the ocean skin. Geophys. Res. Lett. **32:** 1–4. doi:10.1029/2004GL022120.

Capone, D. G., J. P. Zehr, H. Paerl, B. Bergman, and E. J. Carpenter. 1997. Trichodesmium, a globally significant marine cyanobacterium. Science **276:** 1221–1229. doi: 10.1126/science.276.5316.1221.

Carlucci, A. F., D. B. Craven, and S. M. Henrichs. 1985. Surface-film microheterotrophs: Amino acid metabolism and solar radiation effects on their activities. Mar. Biol. **85:** 13–22.

Dafner, E. V., R. Sempéré, N. González, F. Gomez, and M. Goutx. 1999. Cross-slope variations of dissolved organic carbon in the Gulf of Cadiz, North East Atlantic Ocean (February 1998). Mar. Ecol. Prog. Ser. **189:** 301–306.

Dauwe, B., J. J. Middelburg, P. M. J. Herman, and C. H. R. Heip. 1999. Linking diagenetic alteration of amino acids and bulk organic matter reactivity. Limnol. Oceanogr. **44:** 1809–1814.

Del Giorgio, P. A., and J. J. Cole. 2000. Bacterial energetics and growth efficiency, p. 289–325. *In* D. L. Kirchman [ed.], Microbial ecology of the oceans. Wiley-Liss.

De Souza lima, Y. 1985. Dissolved inorganic nutrient enrichment in the sea surface microlayer: Possible effects of abiotic and biotic environmental factors. Oceanol. Acta **8:** 47–58.

Fitznar, H. P., J. M. Lobbes, and G. Kattner. 1999. Determination of enantiomeric amino acids with high-performance liquid chromatography and pre-column derivatisation with o-phthaldialdehyde and N-isobutyrylcysteine in seawater and fossil samples (mollusks). J. Chromatogr. A **832:** 123–132.

Fuhrman, J. 1987. Close coupling between release and uptake of dissolved free amino acids in seawater studied by an isotope dilution approach. Mar. Ecol. Prog. Ser. **37:** 45–52.

Fukuda, R., H. Ogawa, T. Nagata, and I. I. Koike. 1998. Direct determination of carbon and nitrogen contents of natural bacterial assemblages in marine environments. Appl. Environ. Microb. **64:** 3352–3358.

Garrett, W. D. 1967. Organic chemical composition of ocean surface. Deep-Sea Res. I **14:** 221–227.

Gasol, J. M., M. D. Doval, J. Pinhassi, J. I. Calderón-Paz, N. Guixa-Boixereu, D. Vaqué, and C. Pedrós-Alió. 1998. Diel variations in bacterial heterotrophic activity and growth in the Northwestern Mediterranean Sea. Mar. Ecol. Prog. Ser. **164:** 107–124.

Goldman, J. C., D. A. Caron, and M. R. Dennett. 1987. Regulation of gross growth efficiency and ammonium regeneration in bacteria by substrate C : N ratio. Limnol. Oceanogr. **32:** 1239–1252.

González, N., R. Anadón, and L. Viesca. 2003. Carbon flux through the microbial community in a temperate sea during summer: Role of bacterial metabolism. Aquat. Microb. Ecol. **33:** 117–126.

Gordon, L. I., J. C. J. Jennings, A. A. Ross, and J. M. Krest. 1993. A suggested protocol for continuous flow automated analysis of seawater nutrients (phosphate, nitrate, nitrite and silic acid) in the WOCE hydrographic program and the Joint Global Ocean Fluxes Study. Methods Manual WHPO 91-1. WOCE hydrographic progam office.

Hardy, J. T. 1982. The sea surface microlayer: Biology, chemistry and anthropogenic enrichment. Progr. Oceanogr. **11:** 307–328.

Harvey, G. W., and L. A. Burzell. 1972. A simple microlayer method for small samples. Limnol. Oceanogr. **1:** 156–157.

Hatcher, R. F., and B. C. Parker. 1974. Laboratory comparisons of four surface microlayer samplers. Limnol. Oceanogr. **19:** 162–165.

Herndl, G. J., G. Müller-Niklas, and J. Frick. 1993. Major role of ultraviolet-B in controlling bacterioplankton growth in the surface layer of the ocean. Nature **361:** 717–719.

Joux, F., H. Agogué, I. Obernosterer, C. Dupuy, T. Reinthaler, G. J. Herndl, and P. Lebaron. 2006. Microbial community structure in the sea surface microlayer at two contrasting coastal sites in the Northwestern Mediterranean Sea. Aquat. Microb. Ecol. **42:** 91–104.

Kähler, P., and W. Koeve. 2001. Marine dissolved organic matter: Can its C : N ratio explain carbon overconsumption? Deep-Sea Res. I **48:** 49–62.

Kaiser, K., and R. Benner. 2005. Hydrolysis-induced racemization of amino acids. Limnol. Oceanogr. Methods **3:** 318–325.

Karl, D. M., and K. M. Björkman. 2002. Dynamics of DOP, p. 249–366. *In* D. A. Hansell and C. A. Carlson [eds.], Biogeochemistry of the marine dissolved organic matter. Academic Press.

Kirchman, D. 1993. Leucine incorporation as a measure of biomass production by heterotrophic bacteria, p. 509–512. *In* P. F. Kemp, B. F. Sherr, E. B. Sherr and J. J. Cole [eds.], Handbook of methods in aquatic microbial ecology. Lewis Publishers.

Kramer, G. D., C. Pausz, and G. J. Herndl. 2005. Elemental composition of dissolved organic matter and bacterioplankton production in the Faroe-Shetland Channel (North Atlantic). Deep-Sea Res. I **52:** 85–97.

Kroer, N. 1993. Bacterial growth efficiency on natural dissolved organic matter. Limnol. Oceanogr. **38:** 1282–1290.

Kuipers, B., G. J. V. Noort, J. H. Vosjan, and G. J. Herndl. 2000. Diel periodicity of bacterioplankton in the euphotic zone of the subtropical Atlantic Ocean. Mar. Ecol. Prog. Ser. **201:** 13–25.

Kuznetsova, M., and C. Lee. 2002. Dissolved free and combined amino acids in nearshore seawater, sea surface microlayers and foams: Influence of extracellular hydrolysis. Aquat. Sci. **64:** 252–268.

———, ———, and J. Y. Aller. 2004. Enrichment of amino acids in the sea surface microlayer at coastal and open ocean sites in the North Atlantic Ocean. Limnol. Oceanogr. **49:** 1605–1619.

Lemée, R., E. Rochelle-Newall, F. Van Wambeke, M.-D. Pizay, P. Rinaldi, and J.-P. Gattuso. 2002. Seasonal variation of bacterial production, respiration and growth efficiency in the open NW Mediterranean Sea. Aquat. Microb. Ecol. **29:** 227–237.

Liss, P. S., and R. A. Duce. 1997. The sea surface and global change., Cambridge University Press.

Mimura, T., J. C. Romano, and Y. De Souza lima. 1988. Microbiomass structure and respiratory activity of microneuston and microplankton in the northwestern Mediterranean Sea influenced by Rhone River water. Mar. Ecol. Prog. Ser. **49:** 151–162.

Momzikoff, A., A. Brinis, S. Dallot, G. Gondry, A. Saliot, and P. Lebaron. 2004. Field study of the chemical characterization of the top ocean surface using various samplers. Limnol. Oceanogr. Methods **2:** 374–386.

Obernosterer, I., P. Catala, T. Reinthaler, G. J. Herndl, and P. Lebaron. 2005. Enhanced heterotrophic activity in the surface microlayer of the Mediterranean Sea. Aquat. Microb. Ecol. **39:** 293–302.

———, B. Reitner, and G. J. Herndl. 1999. Contrasting effects of solar radiation on dissolved organic matter and its bioavailability to marine bacterioplankton. Limnol. Oceanogr. **44:** 1645–1654.

Pausz, C., and G. J. Herndl. 1999. Role of ultraviolet radiation on phytoplankton extracellular release and its subsequent utilization by marine bacterioplankton. Aquat. Microb. Ecol. **18:** 85–93.

Pérez, M. T., C. Pausz, and G. J. Herndl. 2003. Major shift in bacterioplankton utilization of enantiomeric amino acids between surface waters and the ocean's interior. Limnol. Oceanogr. **48:** 755–763.

Pomeroy, L. R., J. E. Sheldon, and W. M. Sheldon. 1994. Changes in bacterial numbers and leucine assimilation during estimations of microbial respiratory rates in seawater by the precision Winkler method. Appl. Environ. Microb. **60:** 328–332.

Regan, J. D., W. L. Carrier, H. Gucinski, B. L. Olla, H. Yoshida, R. K. Fujimura, and R. I. Wicklund. 1992. DNA as a solar dosimeter in the ocean. Photochem. Photobiol. **56:** 35–42.

Reinthaler, T., K. Bakker, R. Manuels, J. Van Ooijen, and G. J. Herndl. 2006. Fully automated spectrophotometric approach to determine oxygen concentrations in seawater via continuous-flow analysis. Limnol. Oceanogr. Methods **4:** 358–366.

Santinelli, C., G. P. Gasparini, L. Nannicini, and A. Seritti. 2002. Vertical distribution of dissolved organic carbon (DOC) in the Western Mediterranean Sea in relation to the hydrological characteristics. Deep-Sea Res. I **49:** 2203–2219.

Simon, M., and F. Azam. 1989. Protein content and protein synthesis rates of planktonic marine bacteria. Mar. Ecol. Prog. Ser. **51:** 201–213.

Suttle, C. A., A. M. Chan, and J. A. Fuhrman. 1991. Dissolved free amino acids in the Sargasso Sea: Uptake and respiration rates, turnover times, and concentrations. Mar. Ecol. Prog. Ser. **70:** 189–199.

Teira, E., M. J. Pazó, P. Serret, and E. Fernández. 2001. Dissolved organic carbon production by microbial populations in the Atlantic Ocean. Limnol. Oceanogr. **46:** 1370–1377.

Van Wambeke, F., D. Lefèvre, L. Prieur, R. Sempéré, M. Bianchi, K. Oubelkheir, and F. Bruyant. 2004. Distribution of microbial biomass, production, respiration, dissolved organic carbon and factors controlling bacterial production across a geostrophic front (Almeria-Oran, SW Mediterranean Sea). Mar. Ecol. Prog. Ser. **269:** 1–15.

Vidal, M., C. M. Duarte, and S. Agustí. 1999. Dissolved organic nitrogen and phosphorus pools and fluxes in the central Atlantic Ocean. Limnol. Oceanogr. **44:** 106–115.

Williams, P. J. le B., and P. A. Del Giorgio. 2005. Respiration in aquatic ecosystems: History and background, p. 1–17. *In* P. A. Del Giorgio and P. J. le B. Williams [eds.], Respiration in aquatic ecosystems. Oxford Univ. Press.

Williams, P. M., A. F. Carlucci, S. M. Henrichs, E. S. Van Vleet, S. G. Horrigan, F. M. H. Reid, and K. J. Robertson. 1986. Chemical and microbiological studies of sea-surface films in the Southern Gulf of California and off the West Coast of Baja California. Mar. Chem. **19:** 17–98.

Wotton, R. S., and T. M. Preston. 2005. Surface films: Areas of water bodies that are often overlooked. BioSci. **55:** 137–145.

Received: 27 February 2007
Accepted: 3 August 2007
Amended: 14 August 2007